Molecular Dynamics Simulations and Vibrational Spectroscopic Studies of Local Structure in Tetraglyme:Sodium Triflate ($CH_3O(CH_2CH_2O)_4CH_3$:$NaCF_3SO_3$) Solutions

Haitao Dong, Jin-Kee Hyun, Christopher P. Rhodes, Roger Frech,* and Ralph A. Wheeler*

Department of Chemistry and Biochemistry, University of Oklahoma, 620 Parrington Oval, Room 208; Norman, Oklahoma 73019

Received: October 22, 2001; In Final Form: February 21, 2002

An oligomeric model for poly(ethylene oxide), tetraglyme, with $NaCF_3SO_3$ at an ether oxygen:Na^+ ratio of 10:1 was used to represent the amorphous phase of PEO:salt systems in molecular dynamics simulations at 300 K and 400 K. Na^+−tetraglyme interactions were examined by calculating chain dimensions, dihedral angle population distribution, and conformational triad populations of coordinating tetraglyme chains. All results consistently show that the Na^+−ether oxygen coordination induces more compact chains by enforcing a gauche conformation for C−C bonds and introducing a strong preference for tgt conformations in the C−O−C−C−O−C bond sequence. Na^+−O(tetraglyme) and Na^+−O(triflate) radial distribution functions reveal that triflate ions contribute more oxygens (4.9 at 300 K and 5.3 at 400 K) than tetraglyme (2.2 at 300 K and 2.0 at 400 K) to the first coordination shell of Na^+. Populations of aggregates consisting of a triflate ion coordinated to 0−3 Na^+ were available from vibrational spectra and were also calculated from equilibrated trajectories. Both results agree well, and the computational results indicate that Na^+−$CF_3SO_3^-$ association increases with increasing temperature. The results are compared with results from a previously studied tetraglyme:$LiCF_3SO_3$ system. Unlike Li^+ in the tetraglyme:$LiCF_3SO_3$ system, bidentate coordination of Na^+ by $CF_3SO_3^-$ becomes more favorable at the higher temperature, at the expense of monodentate and tridentate coordination.

Introduction

Poly(ethylene oxide) (PEO), due to its ability to solvate a variety of inorganic salts and its potential to form systems with high ionic conductivities, has become a widely used host polymer matrix in solid polymer electrolytes (SPE).[1] Used as the medium between the anode and cathode in high energy-density batteries, SPEs are desirable because they can provide variable geometry, large active area, flexibility of operation, and safety.[2] Polymer-salt matrices with high ionic conductivities are desirable for improving the performance of high energy-density batteries. Ionic conductivities in PEO-based SPE, however, are low at room temperature. For PEO:LiX (X = ClO_4, CF_3SO_3), ionic conductivity is in the range from 10^{-3} to 10^{-4} S/cm at 100 °C, whereas it falls to the range from 10^{-6} to 10^{-8} S/cm at room temperature.[3] This limits the practical operation temperature to the 80−140 °C range. One explanation for this problem is the pure PEO crystalline phase found in PEO:salt complexes at room-temperature blocks some fraction of conduction pathways.[4] Thus, finding SPEs with high conductivities and acceptable mechanical properties at a wider temperature range (encompassing room temperature) is ultimately desired. The ionic transport occurs predominately in the amorphous regions and depends on polymer conformations, ion-polymer interactions, and cation−anion association. Molecular-level understanding of these aspects in polymer:salt complexes will help design polymer matrixes and optimize compositions of the SPE to meet the ultimate goal of a commercialized rechargeable battery technology. Spectroscopy and computer simulations have been employed on PEO-based polymer electrolyte systems to further this goal.

Polymer conformations, particularly conformational changes of PEO upon complexation with metal cations in PEO:NaX (X=Br, I, SCN, BF_4, and CF_3SO_3) and PEO:MSCN (M = K, Rb, and Cs) systems, have been studied by vibrational spectroscopy.[5,6] Salt concentration and chain length effects on the conformational changes for short oligomer:salt complexes such as glyme:MCF_3SO_3 (M = Li, Na, and K, glyme = $CH_3O(CH_2O)_nCH_3$, n = 1,2,3, and 4) have also been studied.[7,8] Raman and infrared vibrational spectroscopies have also been used to investigate ionic association in these PEO:salt and oligomer:salt complexes. For instance, different species of ionic aggregates, including free ions, ion pairs, and large aggregates in the glyme:MCF_3SO_3 complexes have been identified through their spectral signatures in the $-SO_3$ symmetric stretching and the CF_3 symmetric deformation regions of the triflate ion (trifluoromethanesulfonate ion, $CF_3SO_3^-$, hereafter abbreviated as Tf^-) at different temperatures and salt concentrations.[9,10] X-ray diffraction studies have determined crystalline structures of a number of PEO:salts including $P(EO)_3$:LiTf and PEO:NaTf.[11−13] These studies show that the cations are coordinated by both the anions and the oxygens of PEO chains and the coordination number is dependent on the size of the cations and anions. For the ionic association, X-ray absorption fine structure has been used to examine temperature effects on ion pairing in PEO:potassium salt complexes, which shows that the number of ion pairs increases with increasing temperature.[14]

Computer simulations provide a direct way to analyze polymer conformations, polymer-ion interactions, and ionic association at the molecular level and have been applied to PEO:salts complexes. Several molecular dynamics (MD) simulations

* To whom correspondence should be addressed. E-mail: rfrech@ou.edu, rawheeler@ou.edu.

10.1021/jp013914w CCC: $22.00
Published on Web 04/12/2002

of PEO:MX (MX = NaI and LiI) complexes have been performed to examine ionic association.[15−18] Different types of ionic aggregates were identified, and the concentration dependence of ionic association was studied. These studies show that the presence of ionic aggregates, and the sizes of these aggregates grow at higher salt concentrations.[15] Borodin et al. studied structural and conformational properties of PEO:LiI melts with ether oxygen:cation ratios of 48:1, 15:1, and 5:1 at 363 K and 450 K. The results indicated that Li^+ cations are more likely coordinated by oxygen from a single chain at the lower temperature. As temperature increases, more polymer chains are involved in the coordination shell, whereas the coordination number of Li^+ remains same. This work also reported a fewer number of "free" ions observed at the higher temperature.[19] Low molecular weight oligomers of PEO have been used to represent the amorphous phases of the polymer-salt matrix at accessible temperatures. An MD simulation study of diglyme:LiI (diglyme = $CH_3O(CH_2CH_2O)_2CH_3$) reported that the degree of ionic aggregation is greater than in the PEO:LiI system and populations of ionic aggregates are nearly independent of temperature.[20]

In most published MD simulation papers, halide salts were used because of the simplicity of monatomic anions. However, the triflate anion, Tf^-, is more applicable in commercialized batteries than halide ions and is more amenable to spectroscopic studies of the anion environment. Due to the lack of information provided by MD simulations for PEO:MTf (M = metal ions) systems, we performed a series of MD simulations on amorphous tetraglyme ($CH_3O(CH_2CH_2O)_4CH_3$):NaTf samples. In a previous paper, we reported results of tetraglyme:LiTf samples with a 10:1 ether oxygen:Li ratio.[21] Here, we will present conformation changes of tetraglyme upon Na^+-ether oxygen complexation, ionic coordination with ether oxygen and triflate oxygen, and cation−anion association in the tetraglyme:NaTf samples with the same 10:1 ether oxygen:salt ratio. The results are also compared with experiment.

Computational Methods. Our model of tetraglyme:NaTf contains 50 tetraglyme chains, 25 Na^+, and 25 Tf^- ions to satisfy the ether oxygen:salt ratio of 10:1. The initial tetraglyme chain configuration was generated from the known crystal structure for PEO.[22] The Na^+ and Tf^- ions were randomly distributed in the tetraglyme matrix. All parameters of the inter- and intramolecular interactions of tetraglyme and Na^+ ion were taken from the AMBER all-atom force field,[23] whereas their partial charges were obtained from the literature.[24] The Lennard−Jones parameters for triflate ion were also from the AMBER all-atom force field. Partial atomic charges for the triflate ion were derived by a standard procedure. First, we performed hybrid Hartree−Fock/density functional quantum chemical calculations[25] and then used the program CHELPG[26] to perform a least-squares fit to find charges that best reproduce the electrostatic potential on a grid of points. The grid was chosen to include at least 13 000 points spaced 0.3 Å apart and located outside the van der Waals radius of each atom. This procedure has been used by us to determine atomic charges for p-benzoquinones and their semiquinone anions and found to give one-electron reduction potentials within approximately 0.1 eV of their experimental values.[27−29]

Molecular dynamics simulations of the model tetraglyme: NaTf were performed at 300 K and 400 K using the AMBER 5.0 MD program.[30] The temperature was held constant in the NPT and NVT ensembles by the Berendsen coupling algorithm.[31] The bond lengths were constrained by SHAKE algorithm, whereas the valence angles and the dihedral angles remained flexible. Periodic boundary conditions were applied and the particle mesh Ewald (PME) method was used to evaluate the long-range electrostatic interactions.[32,33] A direct-space cutoff of 12 Å was used for Lennard-Jones and the electrostatic potentials for both temperatures. The equations of motion were integrated with a time step of 1 fs. The model was kept at 300 K and 400 K and 1.0 atm for 1 ns in the NPT ensemble calculation. Stable densities were obtained, yielding 1.13 g/cm^3 at 300 K and 1.01 g/cm^3 at 400 K. Further equilibration was continued in the NVT ensemble for 2ns.

To verify that the sample boxes were at equilibrium, total energies and conformational changes were monitored over the last 500 ps of the 2 ns NVT run. Moving average total energies calculated every 10 ps increased 1.0% at 300 K and 0.2% at 400 K over this 500 ps period. Conformational changes (e.g., gauche to trans) occurred every 14.1 ps, on average, around C−C bonds and 17.7 ps around C−O bonds at 300 K and at 400 K, conformations changed every 4.3 ps around C−C bonds and 3.9 ps around C−O bonds. The cosine dihedral angle autocorrelation functions around C−C and C−O bonds were calculated from the molecular trajectories and the relaxation times were 15.9 ps and 16.4 ps at 300 K and 2.8 ps and 2.5 ps at 400 K. Therefore, the sample had reached equilibrium, and an additional 500 ps trajectory was collected for analyses.

Experimental Methods

Tetraglyme, tetraethylene gylcol dimethyl ether, (99%) was obtained from Aldrich and used as received. Sodium trifluoromethanesulfonate, NaTf, (≥97%) was obtained from Fluka and dried at 120 °C in a vacuum oven for 48 h. The reagents were transferred to dry N_2 glovebox (≤1 ppm moisture). Stoichiometric amounts of tetraglyme and NaTf were combined to obtain an ether oxygen:salt ratio of 10:1, which describes the ether oxygen to metal cation ratio. No cosolvent was used to dissolve the salt. The solution was stirred for 48 h, and after a few days, the solution appeared optically cloudy. To determine whether an additional phase was present in the solution, differential scanning calorimetry (DSC) measurements were taken on a Mettler DSC 820 calorimeter from 25 °C to 100 °C at a rate of 10 °C/min under a 87 mL/min nitrogen purge. The samples were sealed in aluminum crucibles in the glovebox. The DSC thermograms showed the presence of an endotherm with a peak at ∼35 °C indicating the presence of an additional phase in the system. Therefore, the tetraglyme:NaTf system is biphasic at 300 K; however, the DSC data indicate that the system at 400 K is a single phase system. Using higher concentrations of NaTf, we were able to isolate a crystalline phase of tetraglyme:NaTf which is reported in a separate publication.[34] The comparison of the molecular dynamics results to the experimental solution results are only attempted at 400 K due to the difficulty of modeling multiple phases present at 300 K.

Mid infrared spectra were recorded on a Bruker IFS66V FTIR under a dry air purge using ZnSe plates. The temperature was controlled (est. ±2 K) using an Omega CN9000A temperature controller and a Harrick temperature cell. Peak fitting was accomplished using a commercial program, (Galactic Grams ver 5.2) using a nonlinear least squares algorithm.

Results and Discussion

A. Tetraglyme Chain Dimensions. The mean-square radius of gyration $\langle S^2 \rangle$ and mean-square backbone end-to-end distance $\langle R^2 \rangle$ describe the spatial extent of polymer chains. In this experiment, these quantities are used to investigate conformational changes of tetraglyme chains which are affected by cation-

TABLE 1: Mean-Square Radius of Gyration, $\langle S^2 \rangle$, Mean-Square Backbone End-to-End Distance, $\langle R^2 \rangle$, and Characteristic Ratio C_n for Pure Tetraglyme, Tetraglyme:NaTf, and Tetraglyme:LiTf Samples at $T = 300$ K and 400 K

	T (K)	$\langle S^2 \rangle$ (Å^2)	$\langle R^2 \rangle$ (Å^2)	C_n
tetraglyme	300	21.3 ± 0.3	142.7 ± 4.3	4.9
	400	20.0 ± 0.4	129.5 ± 6.3	4.4
tetraglyme:NaTf	300	17.6 ± 0.4	88.7 ± 4.8	3.0
	400	17.6 ± 0.6	95.1 ± 8.7	3.3
tetraglyme:LiTf	300	18.2 ± 0.5	101.6 ± 6.4	3.5
	400	18.6 ± 0.8	110.9 ± 10.3	3.8

ether oxygen complexation. $\langle S^2 \rangle$ and $\langle R^2 \rangle$ can be easily calculated from the trajectories in MD simulations. $\langle R^2 \rangle$ can also be directly observed experimentally using techniques such as light scattering and, therefore, provide a way to evaluate the accuracy of the applied force field. For convenience, a quantity called the characteristic ratio, defined as $C_n = \langle R^2 \rangle / nl^2$, where n is the number of backbone bonds, and l^2 is the mean-square bond length, is calculated for comparing polymer chains with different lengths.[35] For a freely jointed polymer chain model, this ratio is theoretically predicted as 1. For a real polymer chain, this ratio may vary because of the presence of intra- and intermolecular forces and will reach a limit as $n \rightarrow \infty$. For example, the C_∞ of PEO in the melt is approximately 5.2.[36] Smith et al. reported C_∞ values of 5.7−5.5 for nearly monodisperse PEO melts at 347−459 K by small-angle neutron scattering.[37] Our pure tetraglyme result gives C_n values of 4.9 at 300 K and 4.4 at 400 K, which are in qualitative agreement with the experimental data and show similar temperature dependence. The $\langle S^2 \rangle$, $\langle R^2 \rangle$, and C_n of tetraglyme chains in pure tetraglyme (taken from a separate publication[38]) are listed in Table 1 at 300 K and 400 K. To examine the effects of cation-ether oxygen complexation on the chain dimensions, tetraglyme:NaTf and tetraglyme:LiTf are also listed in Table 1.

Compared to pure tetraglyme, all values of $\langle S^2 \rangle$ and $\langle R^2 \rangle$ in tetraglyme:MTf (M = Na, Li) are smaller at both temperatures. This indicates that either the intrachain attractions or interchain repulsions are stronger when compared to pure tetraglyme. The complexation between the metal cations and the ether oxygens is one obvious attractive force. The smaller sizes of tetraglyme chains imply that the complexation causes the chains to form a more compact shape. In the two tetraglyme:salts systems, the complexation of sodium ions with ether oxygens results in smaller values of $\langle S^2 \rangle$ and $\langle R^2 \rangle$ than complexation of lithium ions with ether oxygens at both temperatures. The calculated differences are close to the statistical error however and may not be significant. Of further interest are the characteristic ratios of tetraglyme:MTf, which show an opposite temperature dependence to what is found in pure tetraglyme for both systems, C_n increases with temperature. This effect implies that the cation complexation with ether oxygens from the same chains becomes weaker at high temperature. The weakened cation-ether oxygen complexation may be because the cation−anion association (discussed further below) becomes more favorable in the competition of ether oxygens and triflate oxygens for sodium ions.

B. Conformations of Tetraglyme Chains. Conformational analysis provides more detailed information about the tetraglyme chains and complements the preceding chain dimension calculations. In this analysis, dihedral angles of the tetraglyme backbone bonds are calculated to show the chain conformation resulting from the cation-ether oxygen complexation. Each tetraglyme chain has two kinds of dihedral angles. One is a dihedral angle around C−C bonds (an O−C−C−O atom sequence) and the other is around C−O bonds (a C−O−C−C atom sequence). The time-averaged population density distribution of the dihedral angles around the C−C bonds for pure tetraglyme at 400 K is shown in Figure 1 (solid line, θ denotes the dihedral angles). This distribution gives three peaks, with the two bigger peaks at the two ends centered around 75° and 285°and between them a smaller peak centered around 180°. By our definition, the dihedral angles around C−C bonds favor gauche plus (g^+, 0° < θ < 120°) and gauche minus (g^-, 240° < θ < 360°) over trans (t, 120° < θ < 240°) conformations. This is referred to the oxygen gauche effect. In polyether chains, a pendant oxygen atom is known to lower the energy of the gauche conformation despite the Coulombic repulsion between ether oxygens, the so-called gauche effect.[35,39] For the dihedral angles around C−O bonds (not shown), the distributions indicate that the t conformation is predominant. All distributions are symmetric about 180° and therefore neither g^+ nor g^- is favored over the other.

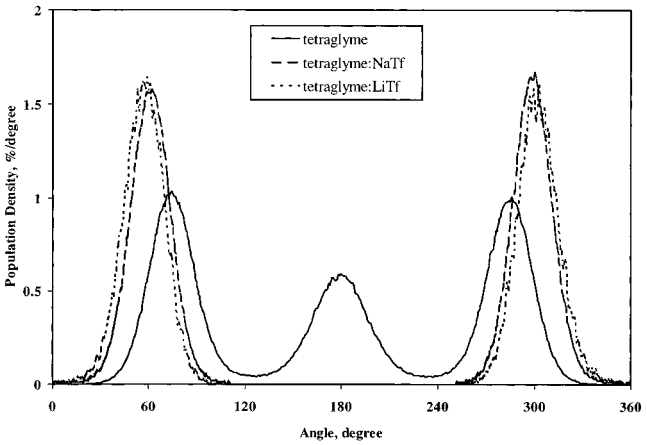

Figure 1. Time-average population density distributions of tetraglyme backbone torsions around C-C bonds in pure tetraglyme (−), tetraglyme:NaTf (---), and tetraglyme:LiTf (···) systems at 400 K.

Because the two adjacent oxygens in one chain can stay in the relatively low-energy gauche conformation, they are in a geometry which allows two oxygens to coordinate a metal cation. The coordination to a metal cation affects the conformation of the O−C−C−O atom sequence as well. To examine the conformational changes, the time-averaged population density distributions of the dihedral angles around the C−C bonds of tetraglyme:NaTf systems at 400 K are also shown in Figure 1 (dashed line). To preferentially investigate conformations of portions of tetraglyme chains that are complexed to sodium ions, we divided the whole chain into two parts, an "inside" region and an "outside" region. The inside region of a chain includes at least two adjacent oxygen atoms that are coordinated to a Na^+, so this portion of a chain forms a local structure of Na^+−O complexation. The outside region is the rest of the chain. If only one oxygen atom of a tetraglyme chain complexes with a Na^+, there should be only an outside region. If all five oxygen atoms of a tetraglyme chain complex with a Na^+, then the whole chain would define only an inside region. It should be noted that only dihedral angles of those O−C−C−O atom sequences in which both oxygens are complexed with the same metal cations (the "inside" regions) are calculated for the population density distributions. Figure 1 shows that g^+ and g^- conformations around C−C bonds are predominant for tetraglyme:NaTf samples. The populations of g^+ and g^- become larger than their populations in pure tetraglyme, whereas the t conformation vanishes for the portions of tetraglyme coordinated to sodium ions. This is because the Na^+−ether oxygen complexation forces the two oxygens to stay in a g^+ or g^-

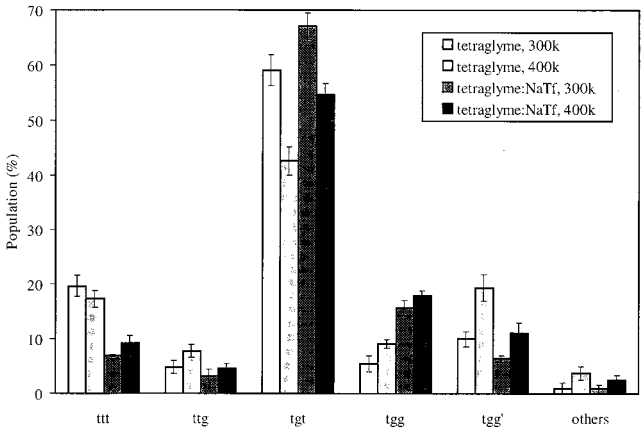

Figure 2. Populations of conformational triads (C-O-C-C-O-C backbone atom sequences) for tetraglyme and tetraglyme:NaTf complex at 300 K and 400 K. Error bars on each column are calculated standard deviations.

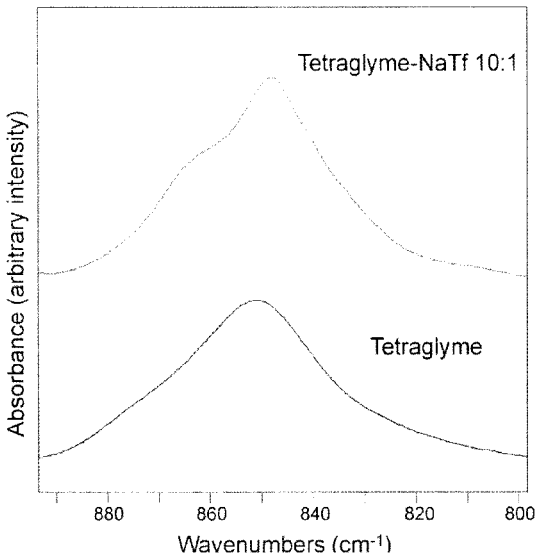

Figure 3. Infrared spectra in the 800−900 cm^{-1} region of tetraglyme and tetraglyme:NaTf 10:1 solutions.

conformation. In the tetraglyme:NaTf, the two distribution peaks of g^+ and g^- are centered around 60° and 300°, instead of 75° and 285° in pure tetraglyme. The shifts of the most probable dihedral angles of the g^+ and g^- conformations clearly show that the Na^+−O complexation forces the two oxygens to be closer to each other to fit in two coordinate positions. To compare different cation species' influence on tetraglyme chain conformations, the distribution of the inside regions in tetraglyme:LiTf is shown in Figure 1 (dotted line). The two distribution peaks of the inside regions in the complexes show very small differences from each other, but the distribution of C−C angles in tetraglyme:LiTf is shifted to a smaller angle (toward the eclipsed state). This may be because the lithium ion's smaller size allows the two oxygens to be even closer to the lithium ion. However, the size does not affect the conformation very much and the complexation of sodium and lithium with ether oxygen shows a very similar influence on tetraglyme chain conformation around the C−C bonds.

Conformational triads are three consecutive dihedral angles along a C−O−C−C−O−C tetraglyme chain sequence. The three dihedral angles are around O−C, C−C, C−O bonds and their dihedral angles, as described in the previous discussion, favor t, g^+(or g^-), and t, respectively. Therefore, the most probable triads for pure tetraglyme should be tg^+t and tg^-t (in this case, g will be used to represent either g^+ or g^- and g′ to indicate a change in sign of the gauche conformation. For example, tgg′ implies either tg^+g^- or tg^-g^+). Populations of tetraglyme triads in pure tetraglyme and in tetraglyme:NaTf at 300 K and 400 K are also shown in Figure 2. To clarify conformational changes upon the Na^+−O complexation, only the tetraglyme chains that participated in the complexation are considered.

In both pure tetraglyme and tetraglyme:NaTf, the tgt conformation is predominant. For pure tetraglyme, the total population of tgt is 59.0% at 300 K and 42.6% at 400 K, and in tetraglyme:NaTf the population of tgt (in the "inside" regions) is 67.0% at 300 K and 54.6% at 400 K. At a given temperature, the population of tgt is higher in tetraglyme:NaTf compared to pure tetraglyme. The preference for the tgt conformation in tetraglyme:NaTf indicates that the Na^+−O complexation favors this local chain conformation. It can be easily understood that a gauche angle around the C−C bond enables the two oxygens to coordinate with Na^+, and the t state implies a further distance between the big end groups and the Na^+ which thus lowers the repulsions. For tetraglyme:NaTf, the tgg and tgg′ conformations have the second (15.7% at 300 K and 17.9% at 400 K) and third largest (6.4% at 300 K and 11.1% at 400 K) populations.

Compared to pure tetraglyme (as observed in Figure 2), the tetraglyme chains that are involved in complexation with Na^+ have more tgg and fewer tgg′ conformations. In our work, the overall ether oxygen:salt ratio of 10:1 is used, but since only complexing tetraglyme chains are considered, the ether oxygen:salt ratio will be more concentrated in these local areas. Andreev et al. reported the crystal structure for a PEO:NaTf complex with ether oxygen:salt ratio of 1:1. The structure shows that the PEO chain adopts a zigzag conformation in which the triads (C−O−C−C−O−C sequence) are tgg.[12] Similarly, the crystalline phase of tetraglyme:NaTf with an ether oxygen:salt ratio of 5:1 shows tgt and tgg conformational sequences, which is consistent with our computational results.[34] Another difference in triads population between pure tetraglyme and tetraglyme:NaTf occurs in the ttt conformation. The Na^+−O complexation decreases its population from 19.7% and 17.3% in pure tetraglyme to 6.9% and 9.2% at 300 K and 400 K, respectively. The ttt conformation is the most extended chain structure and the decrease in its population implies a shorter end-to-end distance for the tetraglyme chains. This is an agreement with the chain dimension results.

Experimental evidence for the conformational changes of tetraglyme due to coordination to cations can be observed in the vibrational spectra. The bands in the 800−1000 cm^{-1} region are particularly sensitive to conformation and have been used in PEO:salt systems to investigate conformational changes induced by the salt.[7,40] IR spectra of pure tetraglyme at 400 K and a tetraglyme:NaTf solution with ether oxygen:salt = 10:1 at 400 K are presented in Figure 3. The spectrum of pure tetraglyme shows a band centered at 851 cm^{-1} and a high frequency shoulder. The band at 851 cm^{-1} is due to ethylene oxide units or sequences which contain gauche O−C−C−O dihedral angles. The spectrum of the tetraglyme:NaTf solution shows a peak centered at 848 cm^{-1} and a defined shoulder at 864 cm^{-1}. The 864 cm^{-1} band is due to predominantly CH_2 wagging and CH_2 twisting motions of C−O−C−C−O−C units or sequences in tgt conformations which interact with sodium atoms, and the band has a fairly weak IR intensity.[9,41] Previous studies have shown that preferred interaction of ethylene oxide units with cations in glyme:salt solutions is for C−O−C−C−O−C bond sequences in trans-gauche-trans conformations.[7] The

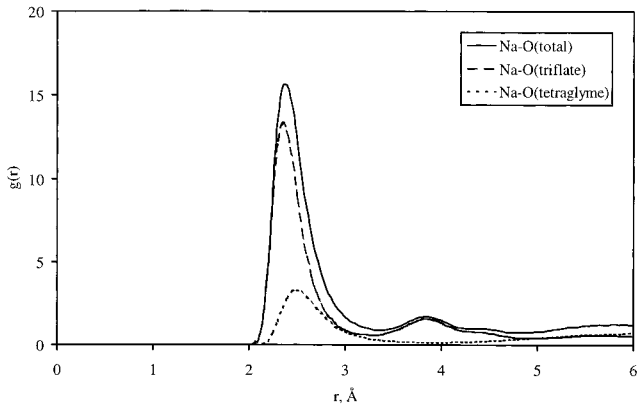

Figure 4. Radial distribution functions (RDF) between Na^+ and all oxygens (—), Na^+ and ether oxygens (···), and Na^+ and triflate oxygens (---) in tetraglyme:NaTf complext at 400 K.

TABLE 2: Coordination Numbers of Na^+ and Li^+ in Tetraglyme:NaTf and Tetraglyme:LiTf Samples at 300K and 400K. the Total Coordination Numbers, the Numbers of Ether Oxygens, and the Numbers of Triflate Oxygens Are Calculated by integrating the appropriate radial distribution functions from zero to the position of the first minimum

	O(total)		O(tetraglyme)		O(triflate)	
T (*K*)	Na^+	Li^+	Na^+	Li^+	Na^+	Li^+
300	7.1	6.2	2.2	1.6	4.9	4.6
400	7.3	6.2	2.0	1.3	5.3	4.8

interaction of the ethylene oxide unit with a sodium ion results in a different O−C−C−O dihedral angle than is present without the sodium atom. The frequency shift of the center of the band from 851 cm^{-1} in pure tetraglyme to 848 cm^{-1} in the tetraglyme:NaTf solution is attributed to the change in the relative populations of different conformers.

C. Na^+−Ether Oxygen Complexation. As seen in crystal structures of PEO:MTf (M = Na, Li) complexes, the cation can complex with oxygen from both the triflate ions and the polyether chains.[11,12] In PEO:NaTf (ether oxygen:salt = 1:1), the total coordination number for Na^+ is six, consisting of four oxygens from four different triflate ions and two oxygens from a polyether chain. In the crystal structure of tetraglyme:NaTf (ether oxygen:salt = 5:1), the total coordination number for Na^+ is seven, consisting of two oxygens from two triflate ions and five ether oxygens from a single tetraglyme chain.[34]

Radial distribution functions (RDF) are used to examine the ether oxygen and triflate oxygen coordination to Na^+ in amorphous tetraglyme:NaTf. The RDFs of Na−O(total), Na−O(triflate), and Na−O(tetraglyme) at 400 K were calculated from the trajectories and are displayed in Figure 4. The Na−O(total) RDF shows a strong first peak at 2.4 Å followed by a minimum at 3.4 Å. The Na−O(triflate) RDF has a similar shape, with Na−O(total) as the first peak and minimum located at 2.4 and 3.2 Å, respectively. The Na−O(tetraglyme) RDF has a much smaller peak at 2.5 Å and no obvious minimum. The first peak positions, the most probable distances between Na^+ and oxygens, are in agreement with the mean Na−O distance of 2.46 Å observed experimentally for crystalline tetraglyme:NaTf.[34]

The larger peak of the Na−O(triflate) RDF suggests that Na^+ is coordinated by more triflate oxygens than tetraglyme oxygens. An integration of the RDFs from zero to the first minimum (the radius of the first coordination shell) provides coordination numbers. All calculated results are listed in Table 2. The total coordination number for Na^+ is 7.3 at 400 K. This coordination number is slightly larger than the six or the seven-coordinated Na^+ in the crystal structures. The results also give an average of 2.0 ether oxygens and 5.3 triflate oxygens coordinating each Na^+. The greater number of triflate oxygens indicates the Na-triflate oxygen complexation is more favorable than Na-ether oxygen complexation. This result qualitatively agrees with the PEO:NaTf crystal structure but is in contrast to the crystalline tetraglyme:NaTf structure with ether oxygen:salt = 5:1 where ether oxygens are more favored than triflate oxygens.

The RDFs of Na−O(total), Na−O(tetraglyme), and Na−O(triflate) at 300 K have a similar shapes (only the first minimum of the Na−O(total) RDF occurs at 3.3 Å, slightly different from 3.4 Å at 400 K) and therefore are not shown. The coordination numbers obtained by integrating these RDFs are listed in Table 2. As the temperature is increased from 300 K to 400 K, the total coordination number increases from 7.1 to 7.3, the contribution of triflate oxygens increases from 4.9 to 5.3, and the contribution of ether oxygens decreases from 2.2 to 2.0. This result suggests that at higher temperatures the triflate oxygens compete more successfully with ether oxygens for Na^+.

This is consistent with the mean-square end-to-end distance results of tetraglyme:NaTf complex presented above. The larger extent of tetraglyme chains at 400 K implies a weaker Na-ether oxygen complexation. This result agrees with the temperature dependence shown by tetraglyme oxygen's coordination numbers.

For comparison with tetraglyme:LiTf samples, which is reported in a previous paper,[21] the coordination numbers of Li^+ are also listed in Table 2. The lithium result also shows a stronger cation-triflate oxygen complexation (4.6 at 300 K and 4.8 at 400 K) than cation-ether oxygen complexation (1.6 at 300 K and 1.3 at 400 K). The temperature dependence of coordination numbers in the two complexes also agrees each other although the coordination numbers of Li^+ are smaller than the corresponding numbers of Na^+. This can be attributed to the lithium ion's smaller size, which does not allow as many coordination sites as the larger sodium ion.

D. Ionic Association. Crystal structure studies of PEO:MTf complexes have shown that the metal ions strongly associate with the SO_3 portion of the triflate ions. For example, in the PEO:NaTf (ether oxygen:salt = 1:1) crystal structure each Na^+ associates with four oxygens from four triflate ions while each triflate ion also associates with four Na^+ ions. In crystalline PEO:NaTf, two of the three oxygens in the SO_3 end of the triflate each coordinate with a Na^+ ion, and the third oxygen bridges two Na^+ ions.[12] In amorphous oligomeric PEO:MTf systems, estimates of the populations of free ion and ion associated species such as ion pairs and aggregates can be obtained from spectroscopic analysis of the symmetric deformation mode of the CF_3 portion in triflate, $\delta_s(CF_3)$, through the dependence of the frequency of the $\delta_s(CF_3)$ mode on the nature of cation−anion association.[10] A partial IR spectrum of tetraglyme:NaTf with an ether oxygen:Na ratio of 10:1 at 400 K is shown in Figure 5. The spectrum can be curve-fit with a linear baseline and four mixed Lorentzian−Gaussian bands at 765, 761, 757, and 753 cm^{-1}, corresponding to the aggregate species $[Na_3Tf]^{2+}$, the triple ion $[Na_2Tf]^+$, the ion pair [NaTf], and the spectroscopically "free" ion Tf^-. The frequencies of these species are consistent with studies of triflate anions coordinated to Li^+ and Na^+ ions in a variety of solvents.[10,42−44] The areas of the four bands are integrated to yield estimates of the populations of these ion associated species and are presented in Table 3.

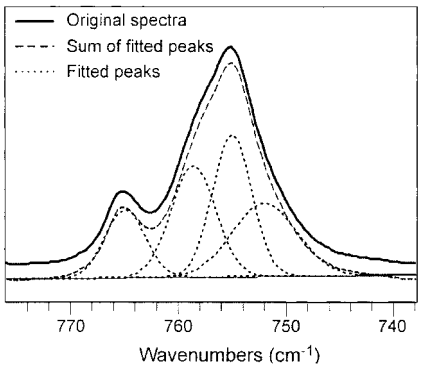

Figure 5. Curve-fit IR spectrum in the 740−780 cm^{-1} region of a tetraglyme-NaTf 10:1 solution indicating the presence of different triflate species "free" triflate ions (Tf^-) at 752 cm^{-1}, ion-pairs ([NaTf] at 755 cm^{-1}, aggregate species ($[Na_2Tf]^+$) at 758 cm^{-1} and aggregate ($[Na_3Tf]^{2+}$) at 765 cm^{-1}.

TABLE 3: Comparison of Calculated Populations of Na^+-Tf^- Associated "Anion Aggregates" (see text) in Tetraglyme:NaTf Samples from MD Results at 300 K and 400 K with IR Experimental Data at 398 K in Parentheses

T (K)		Tf^-	MTf	$[M_2Tf]^+$	$[M_3Tf]^{2+}$
300	Na	42	40	15	3
	Li	20	46	28	6
400	Na	9(24)	39(23)	38(35)	13(13)
	Li	18	44	30	8

MD results for tetraglyme:LiTf samples are also listed for comparison. The 'M' in the species names denotes metal ions (either Li^+ or Na^+).

The populations of ionic species are also calculated from the trajectories collected in MD simulations of the tetraglyme:NaTf sample. To investigate Na^+-Tf^- association, we examined structure from the perspective of the cation and the anion separately. We count the number of sodium ions around a triflate anion by using the first peak positions of the Na−O(triflate) RDFs, 2.5 Å at both temperatures. All IR (in parentheses) and MD results are summarized in Table 3. At 300 K, the "free" triflate ion and the ion pair are the predominant species in tetraglyme:NaTf samples as they account for 42% and 40% of the total ion associated species. The triple ion has 15% of the total population and only a very small amount (3%) of $[Na_3Tf]^{2+}$ aggregates is found. However, the populations of these species change dramatically as temperature increases. Only 9% of total species are found to be "free" triflate ions at 400 K. The ion pair still has a large population, 39% (40% at 300 K), whereas the triple ion and the $[Na_3Tf]^{2+}$ aggregates demonstrate a large growth in their populations: from 15% to 38%, and 3% to 13%, respectively. The changes indicate that the cation−anion association becomes more extensive at higher temperature. This agrees with the coordination number calculations and the chain dimension results. The results from two methods, MD simulations and IR spectroscopy, show some inconsistency for the "free" ion and ion pair, but agree well for the more highly associated species.

The populations of triflate anion species in tetraglyme:LiTf samples calculated from MD trajectories are also listed in Table 3. These populations agree very well with IR results.[21] Among all ionic species, the Li^+-Tf^- ion pair is the most populous species (46% at 300 K, 44% at 400 K). The next most populous species are the triple ion (28%), the "free" triflate ion (20%), and the aggregate (6%) at 300 K. Their populations change slightly at 400 K, as they are 30%, 18%, and 8%, respectively. In tetraglyme:NaTf there are more "free" ions (42%) than triple ions (15%) at 300 K, whereas in tetraglyme:LiTf there are more triple ions (38%) than "free" ions (9%). However in tetraglyme:NaTf aggregation appears highly temperature dependent, but in tetraglyme:LiTf the populations of Li^+-Tf^- species show only a slight temperature dependence.

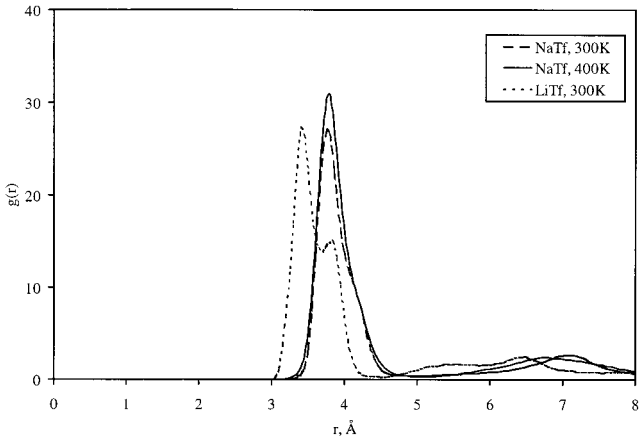

Figure 6. Radial distribution functions (RDF) between Na^+ and the triflate center of mass in tetraglyme:NaTf complex at 300 K (---) and 400 K (—). A RDF between Li^+ and the triflate center of mass in tetraglyme:LiTf complex at 300 K (•••, adopted from ref 21) is shown for comparison.

TABLE 4: Coordination Geometries for Na Coordinated to Triflate in Tetragylme:NaTf Samples Calculated from MD Trajectories at 300 K and 400 K

	NaTf	$[NaTf_2]^-$	
T (K)	(mono)	(mono,tri)	(bi,bi)
300	3.4 ± 0.3	11.1 ± 0.5	13.5 ± 0.7
400	0	0.6 ± 0.4	20.7 ± 2.1

	$[NaTf_3]^{2-}$			
T (K)	(mono,mono,bi)	(mono,bi,bi)	(mono,bi,tri)	(bi,bi,bi)
300	15.1 ± 0.5	9.5 ± 0.4	11.3 ± 1.0	6.6 ± 0.4
400	11.6 ± 2.6	17.8 ± 2.4	5.2 ± 0.9	15.5 ± 3.5

Three species, the NaTf ion pair, $[NaTf_2]^-$, and $[NaTf_3]^{2-}$, are found for the system. The association geometries between Na^+ and triflate oxygens are listed in parentheses. Mono, bi, and tri denote monodentate, bidentate, and tridentate coordination geometries, respectively. Only geometries with significant temperature dependence are listed.

Radial distribution functions between Na^+ and the triflate ion's center of mass are calculated and shown in Figure 6. These functions are expected to give more information of the Na^+-Tf^- association. In our previous study of tetraglyme:LiTf system, the Li^+- Tf center of mass RDF showed an interesting feature, as there was a strong first peak followed by a smaller peak at both 300 K and 400 K. After further study, the two peaks turned out to be two distinguishable Li^+−Tf^- coordination geometries, the bidentate and the monodentate structure. The bidentate geometry was more populous in tetraglyme:LiTf. In tetraglyme:NaTf, each of the Na^+-center of mass of triflate RDFs at 300 K (solid line) and 400 K (dashed line) gives a big peak at 3.8 Å with an indistinct shoulder.

A population analysis for cation environment has been done to further address the question of ionic association geometries. In contrast to the analysis from the triflate ion's point of view presented above, the populations shown in Table 4 focus on how many triflate ions are around a Na^+ and what kind of geometry is formed between the Na^+ and the triflate's three oxygens. The cutoff value used in this calculation is 3.4 Å, the first minimum of Na^+−O(triflate) RDFs. It should be noticed that this cation environment analysis only considers triflate anions which are in the first coordination shell of Na^+. Some

of the triflate anions around the Na^+ are coordinated to other Na^+ ions and, therefore, possibly form more complicated ionic aggregates with several cations and anions. The result shows that the aggregate, $[NaTf_3]^{2-}$, is the dominant aggregate with 52.0% of the population at 300 K and 58.9% at 400 K, whereas the triple ion, $[NaTf_2]^-$, is second most populous with 36.4% at 300 K and 33.1% at 400 K. The NaTf ion pair accounts for the rest of the population. The highly associated species $[NaTf_3]^{2-}$ becomes more highly populated at 400 K indicating that the cation−anion association is favored with increasing temperature.

For each of the aggregates, details of the Na^+−triflate oxygen aggregate geometries are summarized in Table 4. Mono, bi, and tri in the parentheses means that the Na^+ associates with oxygens through a mono, bi, and tridentate geometry, respectively. In the NaTf pair, the monodentate geometry disappears at 400 K, whereas the bidentate and tridentate remain unchanged (Geometries with no significant temperature dependence are not listed in the table). In $[NaTf_2]^-$, the population of (mono,tri) coordination dramatically decreases from 11.1% to 0.6% at 400 K. Meanwhile, the (bi,bi) coordination becomes more highly populated (20.7%, comparing to 13.5%) with increasing temperature. In $[NaTf_3]^{2-}$, populations of (mono,mono,bi) and (mono,bi,tri) decrease at high temperature. But (mono,bi,bi) and (bi,bi,bi) show an opposite temperature dependence as their populations increase from 9.5% to 17.8% and from 6.6% to 15.5%, respectively. In general, this population analysis shows that the higher temperature favors the bidentate Na^+−Tf^- association geometry.

Conclusions

Molecular dynamics simulations and vibrational spectroscopy are used to investigate structural properties of the tetraglyme:NaTf system with an ether oxygen:salt ratio of 10:1 at 300 and 400 K. Mean-square radii of gyration and end-to-end distances of tetraglyme chains are calculated from the MD simulations. Smaller values of these quantities for tetraglyme chains coordinating Na^+ at both temperatures suggest that the tetraglyme chains form more compact shapes upon Na^+−ether oxygen complexation. The population density distributions of dihedral angles around C−C bonds in tetraglyme from the MD simulations are found to favor the gauche (g^+ or g^-) over the trans (t) conformation, whereas the dihedral angles around C−O bonds favor the t more than the g^+ and g^- conformations. Upon Na^+−ether oxygen complexation, dihedral angles around C−C bonds in which both oxygens coordinate to the same Na^+ (defined as the inside regions) show predominant g^+ and g^- conformations, whereas the t conformation vanishes. Moreover, the most probable values of those angles are shifted from noncoordinating tetraglyme's 75° (g^+) and 285° (g^-) to 60° and 300°. The population analysis of the conformational triads (C−O−C−C−O−C sequences) in tetraglyme chains shows that tgt is the most populous conformation (59.0%). The tgt conformation is stabilized by the Na^+−ether oxygen complexation as its population increases to 67.0% in tetraglyme:NaTf at 300 K. At higher temperature, the tgt conformation in tetraglyme:NaTf decreases to 54.6%, implying that the Na^+-ether oxygen complexation is less favored at the high temperature.

The coordination numbers of Na^+ are calculated by integrating Na^+−O(triflate) and Na^+−O(tetraglyme) radial distribution functions (RDFs). Overall, the sodium ions are coordinated by approximately seven oxygens (7.1 oxygen atoms at 300 K and 7.3 at 400 K). The triflate oxygens are clearly the major contributors to the first coordination shell (4.9 at 300 K) and become even more favored (5.3) at 400 K. Meanwhile, the ether oxygen's contribution decreases from 2.2 to 2.0 with increasing temperature. A comparison of the Na^+ coordination calculated in this work with the two crystal structures relevant to this work is a bit surprising. In the MD results, the sodium ion is coordinated to 2.2 ether oxygen atoms and 4.9 triflate oxygen atoms at 300 K. As noted earlier, this is consistent with the crystal structure of P(EO):NaTf wherein the sodium ion is coordinated to 2 ether oxygen atoms and 4 triflate oxygen atoms. However, this stands in sharp contrast to the single crystal structure of tetraglyme:NaTf, where the sodium ion is coordinated to 5 ether oxygen atoms and two triflate oxygen atoms. We had expected that if a significant difference between MD and crystal structure results would occur, the discrepancy would be with the high molecular weight PEO system because of the relatively greater difficulty in packing a continuous polyether chain into the crystal. However, a closer examination of the tetraglyme:NaTf crystal structure shows chains of sodium ions completely "wrapped" by all oxygen atoms of a tetraglyme molecule with triflate ions bridging adjacent "wrapped" cations. Therefore, the crystal structure of the tetraglyme system is most unusual and quite unrelated to the structure of the high molecular weight PEO system that our MD simulation more closely mimics.

A number of IR bands have been assigned for Na^+-Tf^- association species in tetraglyme:NaTf systems and their populations are obtained by integrating the areas. The results from MD simulations agree well with IR experiments for $[Na_2Tf]^+$and $[Na_3Tf]^{2+}$ at 400 K. The MD calculations also show that the population of free ions, Tf^-, dramatically decreases from 42% to 9% with increasing temperature, whereas $[Na_2Tf]^+$ and $[Na_3Tf]^{2+}$ increase from 15% to 38% and from 3% to 13%, respectively. The ion pair, [NaTf], remains the most populous species at both temperatures (40% at 300 K and 39% at 400 K). Compared to tetraglyme:LiTf system (presented previously),[21] tetraglyme:NaTf has more "free" Tf^- at 300 K and more $[Na_2Tf]^+$and $[Na_3Tf]^{2+}$ at 400 K.

Monodentate, bidentate and tridentate coordination geometries of Na^+ by Tf^- were identified. For Na^+ which is coordinated to two triflate ions, $[NaTf_2]^-$, a distribution of coordination geometries exists and a double-bidentate geometry in which the Na^+ bridges four oxygens, two from each triflate ion, is favored at the higher temperature. In $[NaTf_3]^{2-}$, Na^+−Tf^- association through mono-bi-bidentate and bi-bi-bidentate geometries becomes more prominent with increasing temperature. It is important to emphasize that the notation of $[NaTf_2]^-$ and $[NaTf_3]^{2-}$ includes only triflate anions which are in the first coordination shell of Na^+. Some of the triflate anions in these species are coordinated to other Na^+ ions, and therefore exist as part of ionic aggregates rather than as isolated species. The percentages of these association geometries as a function of temperature show that the bidentate structure is favored at the higher temperature.

Acknowledgment. This work was partially supported by funds from the Oklahoma Center for the Advancement of Science and Technology, Contract No. 5377 and by a grant of supercomputer time from the National Science Foundation/National Computational Science Alliance, award number MCA96-N019. We thank Scott E. Boesch for providing force field parameters for the triflate anion.

References and Notes

(1) MacCallum, J. R.; Vincent, C. A. *Polymer Electrolyte Reviews*; Elsevier: New York, 1987; Vol. 1, 2.

(2) Gray, F. M. *Solid Polymer Electrolytes. Fundamentals and Technological Applications*; VCH: New York, 1991.
(3) Albinsson, I.; Mellander, B.-E.; Stevens, J. R. *Polymer* **1991**, *32*, 2712−2715.
(4) Bruce, P. G.; Vincent, C. A. *J. Chem. Soc., Faraday Trans.* **1993**, *89*, 3187−3203.
(5) Papke, B. L.; Ratner, M. A.; Shriver, D. F. *Chem. Solids* **1981**, *42*, 493−500.
(6) Dupon, R.; Papke, B. L.; Ratner, M. A.; Whitmore, D. H.; Shriver, D. F. *J. Am. Chem. Soc.* **1982**, *104*, 6247−6251.
(7) Frech, R.; Huang, W. *Macromolecules* **1995**, *28*, 1246−1251.
(8) Bernson, A.; Lindgren, J.; Huang, W.; Frech, R. *Polymer* **1995**, *36*, 4471−4478.
(9) Frech, R.; Huang, W. *Solid State Ionics* **1994**, *72*, 103−107.
(10) Huang, W.; Frech, R.; Wheeler, R. A. *J. Phys. Chem.* **1994**, *98*, 100−110.
(11) Lightfoot, P.; Mehta, M. A.; Bruce, P. G. *Science* **1993**, *262*, 883−885.
(12) Andreev, Y. G.; MacGlashan, G. S.; Bruce, P. G. *Phys. Rev. B* **1997**, *55*, 12 011−12 017.
(13) Bruce, P. G. *Electrochim. Acta* **1995**, *40*, 2077−2085.
(14) Yang, X. Q.; Lee, H. S.; McBreen, J.; Xu, Z. S.; Skotheim, T. A.; Okamoto, Y.; Lu, F. *J. Chem. Phys.* **1994**, *101*, 3230−3233.
(15) Muller-Plathe, F.; van Gunsteren, W. F. *J. Chem. Phys.* **1995**, *103*, 4745−4756.
(16) Londono, J. D.; Annis, B. K.; Habenschuss, A.; Borodin, O.; Smith, G. D.; Turner, J. Z.; Soper, A. K. *Macromolecules* **1997**, *30*, 7151−7157.
(17) Payne, V. A.; Xu, J.-h.; Forsyth, M.; Ratner, M. A.; Shriver, D. F.; de Leeuw, S. W. *J. Chem. Phys.* **1995**, *103*, 8734−8745.
(18) Payne, V. A.; Xu, J.-H.; Forsyth, M.; Ratner, M. A.; Shriver, D. F.; de Leeuw, S. W. *J. Chem. Phys.* **1995**, *103*, 8746−8755.
(19) Borodin, O.; Smith, G. D. *Macromolecules* **1998**, *31*, 8396−8406.
(20) Borodin, O.; Smith, G. D. *Macromolecules* **2000**, *33*, 2273−2283.
(21) Hyun, J.-K.; Dong, H.; Rhodes, C. P.; Frech, R.; Wheeler, R. A. *J. Phys. Chem. B* **2001**, *105*, 3329−3337.
(22) Takahashi, Y.; Tadokoro, H. *Macromolecules* **1973**, *6*, 672−675.
(23) Cornell, W. D.; Cieplak, P.; Bayly, C. I.; Gould, I. R.; Merz, K. M.; Ferguson, D. M.; Spellmeyer, D. C.; Fox, T.; Caldwell, J. W.; Kollman, P. A. *J. Am. Chem. Soc.* **1995**, *117*, 5179−5197.
(24) Muller-Plathe, F. *Acta Polymer.* **1994**, *45*, 259−293.
(25) Boesch, S. E.; Wheeler, R. A. **2001**, unpublished work.
(26) Breneman, C. M.; Wiberg, K. B. *J. Comput. Chem.* **1990**, *11*, 361−373.
(27) Wheeler, R. A. *J. Am. Chem. Soc.* **1994**, *116*, 11 048−11 051.
(28) Raymond, K. S.; Grafton, A. K.; Wheeler, R. A. *J. Phys. Chem. B* **1997**, *101*, 623−631.
(29) Wise, K. E.; Grafton, A. K.; Wheeler, R. A. *J. Phys. Chem. A* **1997**, *101*, 1160−1165.
(30) Case, D. A.; Pearlman, D. A.; Caldwell, J. W.; Cheatham III, T. E.; Ross, W. S.; Simmerling, C. L.; Darden, T. A.; Merz, K. M.; Stanton, R. V.; Cheng, A. L.; Vincent, J. J.; Crowley, M.; Ferguson, D. M.; Radmer, R. J.; Seibel, G. L.; Singh, U. C.; Weiner, P. K.; Kollman, P. A. *AMBER 5*; University of California-San Francisco: San Francisco, 1997.
(31) Berendsen, H. T. C.; Postma, J. P. M.; van Gunsteren, W. F.; DiNola, A.; Haak, J. R. *J. Chem. Phys.* **1984**, *81*, 3684−3690.
(32) Darden, T.; York, D.; Pedersen, L. *J. Chem. Phys.* **1993**, *98*, 10 089−10 092.
(33) Essmann, V.; Perera, L.; Berkowitz, M.; Darden, T.; Lee, H.; Pedersen, L. *J. Chem. Phys.* **1995**, *103*, 8577−8593.
(34) Rhodes, C. P.; Khan, M.; Frech, R., in preparation.
(35) Flory, P. J. *The Statistical Mechanics of Chain Molecules*; Hanser: New York, 1988.
(36) Kawaguchi, S.; Imai, G.; Suzuki, J.; Miyahara, A.; Kitano, T.; Ito, K. *Polymer* **1997**, *38*, 2885−2891.
(37) Smith, G. D.; Yoon, D. Y.; Jaffe, R. L.; Colby, R. H.; Krishnamoorti, R.; Fetters, L. J. *Macromolecules* **1996**, *29*, 3462−3469.
(38) Dong, H.; Hyun, J.-K.; Durham, C.; Wheeler, R. A. *Polymer* **2001**, *42*, 7809−7817.
(39) Abe, A.; Mark, J. E. *J. Am. Chem. Soc.* **1976**, *98*, 6468−6476.
(40) Matsuura, H.; Fukuhara, K. *J. Polym. Sci. B* **1986**, *24*, 1383−1400.
(41) Boesch, S. E.; Rhodes, C. P.; Frech, R.; Wheeler, R. A. *Phys. Chem. Commun.* **2002**, in preparation.
(42) Frech, R.; Huang, W. *J. Solution Chem.* **1994**, *23*, 469−481.
(43) Frech, R.; Huang, W.; Dissanayake, M. A. K. L. *Mater. Res. Soc. Symp. Proc.* **1995**, *369*, 523−534.
(44) Rhodes, C. P.; Frech, R. *Solid State Ionics* **1999**, *121*, 91−99.